ESAT-6 of *Mycobacterium tuberculosis* downregulates cofilin1 and reduces the phagosome acidification in infected macrophages

P P Mahesh[1], R J Retnakumar[1], Sivakumar K C[2] and Sathish Mundayoor[1]*

Author addresses and affiliation

1 Mycobacteria Research, Bacterial and Parasite Disease Biology, Rajiv Gandhi Centre for Biotechnology, Thycaud P.O., Trivandrum 695014, Kerala, India

2 Genomics Core Facility, Rajiv Gandhi Centre for Biotechnology, Thycaud P.O., Trivandrum 695014, Kerala, India

Email: ppmahesh1982@gmail.com, retnakumarrj@rgcb.res.in, sivakumar@rgcb.res.in, *sathish.mundayoor@gmail.com (Correspondence)

Abstract

Mycobacterium tuberculosis when phagocytosed by macrophages is not cleared completely and many of the bacteria remain in phagosomes indefinitely. In this study we considered abnormal retention of filamentous actin on early phagosomes contributing to defective phagosome acidification. Phosphocofilin1, the inactive form of actin depolymerizing protein cofilin1, which leads to retention of filamentous actin, and the total filamentous actin itself were found upregulated in macrophages infected with virulent *M. tuberculosis*. Over expression of constitutively active cofilin1 in macrophages was found to increase phagosome acidification when infected with virulent *M. tuberculosis*. The anticancer drug sorafenib which activates cofilin1 in PI3K dependent manner was also found to increase phagosome acidification. Cofilin1, known to be positively regulated by superoxide was found to be downregulated by ESAT-6 of *M. tuberculosis* where the latter is known to reduce ROS in macrophages. Ectopic expression of ESAT-6 in macrophages was found to increase filamentous actin and to transform the macrophages more spindle shaped. ESAT-6 was also found to decrease phagosome acidification in macrophages infected with an avirulent *M. tuberculosis* strain. Finally, this study proposes a role for the amino acid methionine in resisting ROS by creating M93 mutants of ESAT-6.

Introduction

Tuberculosis still remains a global health concern and claims lakhs of deaths every year especially in third world countries. The virulent *M. tuberculosis* (Mtb), after entry in to macrophages, escapes phagosome-lysosome fusion and resides in the immature phagosome indefinitely[1]. The present study considers abnormal retention of filamentous actin on early phagosomes contributing to defective phagosome acidification. Actin filaments have critical role in phagocytosis (formation of phagocytic cup), movement of endosomes and their fusion. But retention of excessive actin on phagosomes was reported to prevent phagosome-lysosome fusion[2]. The presence of actin on late phagosomes in virulent *M. tuberculosis* infection was shown to cause inadequate acquisition of the proton pump, V-ATPase by phagosome and inhibiting phagosome maturation[3].

Our study started when a differential expression of the actin depolymerizing protein, cofilin1, was observed in an Mtb infection experiment. Cofilin1 is one of the actin binding proteins having a pivotal role in actin dynamics[4, 5]. Actin dynamics is necessary for diverse cellular functions including phagocytosis, movement of different endosomes and their fusion. Cofilin depolymerizes and severs filamentous actin (F-actin) which releases monomeric actin (G-actin) and also produces actin barbed ends which in turn serves for actin nucleation to form new filaments or creates actin branches. Cofilin1 is an 18kDa protein which is inactivated by Serine-3 phosphorylation. Serine-3 phosphorylated cofilin is not able to bind with actin. A coat of filamentous actin was found to prevent clustering of late endosomes and artificially targeting cofilin1 to late endosomes cleared the filamentous actin coat[6].

Cofilin1 is a stimulus responsive regulator of actin dynamics[7]. Dephosphorylation/activation of cofilin by various pro-inflammatory stimuli and hydrogen peroxide treatment were described earlier[8]. In a recent study we have mentioned that downregulating reactive oxygen species (ROS) may drive the macrophages to a more anti-inflammatory phenotype[9] and confirmed that an abundantly secreted protein of Mtb namely Early Secreted Antigenic Target-6kDa (ESAT-6) downregulates ROS in macrophages. The present study investigates the effect of ESAT-6 on cofilin1, filamentous actin and phagosome acidification. Finally, we propose a role for the amino acid methionine in resisting ROS by ESAT-6.

Results

Mycobacterium tuberculosis downregulates cofilin1 in macrophages

Macrophage monolayers were infected with either live virulent *M. tuberculosis*, H37Rv or heat-killed H37Rv at MOI-1:20 setting uninfected macrophages as control. Total protein was isolated 24h post infection and resolved by 2DE (Fig. 1a). A protein which was downregulated in live H37Rv- infected macrophages compared to heat-killed H37Rv-infected macrophages was identified as cofilin1(non-muscle isoform) by MALDI-TOF-TOF. To confirm the differential expression of cofilin, quantitative real time PCR (RT-PCR) and Western blot (WB) were done

(Fig. 1b & 1c), and results similar to that in 2DE were obtained. Also, WB showed that the expression of cofilin1 in the avirulent Mtb strain H37Ra-infected macrophages was similar to the expression in heat-killed H37Rv-infected macrophages (Fig. 1c). Further, phosphorylation of cofilin1 in macrophage was checked by WB under the infection conditions described earlier using an antibody specific to Serine-3 phosphorylated cofilin1. Phosphorylation of cofilin1 was found to be upregulated in live H37Rv-infected macrophages compared to both heat-killed H37Rv-infected and H37Ra-infected macrophages (Fig. 1c). The above results show that live virulent Mtb downregulates cofilin1 expression and also inactivate it by increasing its phosphorylation in macrophages compared to non-pathogenic infection conditions. Even though a significant change in expression of cofilin1 is seen around 24h post infection, a significant difference in phosphorylation is visible at zero hour of infection -4h after addition of bacteria to macrophages (Fig. 1d).

Cofilin1 is phoshorylated by Lim kinases (LimK1 and LimK2) and dephosphorylated by SSH and cronophin. The expression of LimK1 and phospho (T-508) LimK1- activated LimK1, were checked in different infection conditions. Both LimK1 and pLimK1 were upregulated in live H37Rv-infected macrophages compared to heat-killed H37Rv-infected and H37Ra- infected macrophages (Fig. 2).

Cofilin1 and another actin binding protein Coronin competitively bind with actin. This binding depends on the nucleotide state of actin. Cofilin1 preferably binds to ADP-bound old actin filaments and severs them while Coronin preferably binds to ATP-bound new actin filaments and stabilize them[10, 11]. Further, Coronin is present on mycobacterial phagosomes[12]. Coronin was found to be upregulated in live H37Rv-infected macrophages compared to heat-killed H37Rv-infected and H37Ra-infected macrophages (Fig. 2).

Connecting Cofilin to phagosome acidification/phagosome-lysosome fusion

Since cofilin1 is an actin depolymerizing protein and an abnormal retention of filamentous actin on early phagosomes is known to reduce phagosome acidification, we first looked in to the filamentous actin content of macrophages in different infection conditions. We could observe an increase in F-actin/G-actin ratio in live H37Rv-infected macrophages compared to heat-killed H37Rv-infected and H37Ra-infected macrophages (Fig.3a). By connecting this observation to an earlier study which showed slower movement of lysosomes in virulent Mtb- infected macrophages compared to non-pathogenic Mycobacteria-infected macrophages[13], we speculate that the increase in F-actin is a critical event to cause impaired phagosome processing in virulent Mtb-infected macrophages.

We checked the distribution of F-actin using the F-actin binding dye Phalloidine and phagosome acidification using the probe Lysotracker Red in virulent strain H37Rv-infected, heat-killed H37Rv-infected and avirulent strain H37Ra-infected macrophages 24h post infection. A widespread and rich distribution of F-actin was observed in H37Rv-infected macrophages

compared to other conditions (Fig. 3b). Further, phagosome acidification was found to be very less in H37Rv-infected macrophages compared to other conditions as known earlier (Fig. 4).

Cofilin1 was reported to be dephosphorylated by the broad spectrum kinase inhibitor and anticancer drug sorafenib[14] and the mechanism of this dephosphorylation/activation of cofilin1 was found to be Phosphatidylinositol-3-kinase (PI3K) dependent activation of cofilin1 phosphatase SSH (Sling Shot Homologue). This study also showed a thinned F-actin network in sorafenib-treated cells. We treated the macrophages with 5µM sorafenib after phagocytosis of bacteria (4h after addition of bacteria) and found that F-actin mesh was thinned in H37Rv-infected macrophages which otherwise showed rich F-actin as described earlier (Fig. 5).

Further, the phagosome acidification greatly increased in sorafenib-treated H37Rv-infected macrophages (Fig. 6). These effects of sorafenib were reversed when the sorafenib-treated macrophages were treated along with the PI3K inhibitor wortmannin. We also took the colony count of H37Rv-infected macrophages treated with 5µM sorafenib. In this case sorafenib was added one day after infection to allow the establishment of infection by the virulent bacteria and continued the treatment for another two days. The colony count from sorafenib-treated macrophages was significantly lower than that from the untreated control (Fig. 7a). Since sorafenib is a pro-apoptotic drug there is considerable cell death (Fig. 7b) of macrophages treated with 5µM sorafenib (as acalculated by MTT assay), and 7.5 µM and 10µM concentrations of sorafenib drastically increased the cell death.

To further strengthen the above observations, we constructed a pIRES plasmid bearing constitutively active cofilin1 -S3A mutant, Addgene[15] with ECFP reporter downstream of the gene. Since Serine-3 phoshorylation inactivates cofilin1, the mutation from serine to alanine will turn cofilin1 readily active. The macrophages transfected with cofilin1 mutant or control plasmid were infected with H37Rv, and both F-actin distribution and phagosome acidification were checked 24h post infection. A significant thinning of F-actin mesh (Fig. 8a) and increased phagosome acidification (Fig. 8b) was found in cofilin1 mutant plasmid- transfected macrophages compared to control plasmid-transfected macrophages.

Is cofilin1 a target of pro-inflammatory signaling of macrophages?

Since cofilin1 is known for being positively regulated by ROS and proinflammatory stimuli we checked this in our case. We treated live H37Rv-infected macrophages with different agents of pro-inflammatory nature and did WB to check the expression of cofilin1, pCofilin1, LimK1, pLimK1 and coronin. The reagents used were H_2O_2, TNFα, sorafenib and vitamin D (vitamin D was reported earlier to increase cofilin expression[16] and it is proven host protective in TB). Uninfected macrophages were also treated with *E. coli* LPS. Even though there was not a convincing change in expression of cofilin in the given treatments, there was a considerable dephosphorylation of cofilin1 in all treatments of infected macrophages (Fig. 9). This means that cofilin1 is readily dephosphosphorylated by various pro-inflammatory stimuli. The expression of

LimK1 was reduced in infected macrophages treated with H_2O_2, TNFα and sorafenib while the level of pLimK1 was significantly reduced in all treatments (Fig. 9). Coronin expression was also reduced significantly in all treatments of infected macrophages (Fig. 9).

Secondly, we treated heat-killed H37Rv-infected macrophages with different agents of anti-inflammatory nature and did WB as stated above. The reagents used were ROS scavenger NAC, NF-κB inhibitor PDTC and NOX inhibitor DPI. Expression of cofilin1 was found to be reduced and the level of pCofilin1 was found to be increased in all treatments of infected macrophages (Fig. 10a). LimK1 expression was found to be increased in NAC treatment and the level of pLimK1 was found to be increased in all treatments of infected macrophages (Fig. 10b). We could not observe a significant change in expression of coronin in any of the above listed treatments (Fig. 10c).

Effect of ESAT-6 of *Mycobacterium tuberculosis* on actin and cofilin1: proposing a mechanism of action for ESAT-6

Earlier studies showed that Mtb ESX secretory system and its effectors cause phagosome maturation arrest in infected macrophages[17]. Another study shows that ectopic expression of ESAT-6 in *Dictyostelium* induces the formation of an F-actin coat around Mtb phagosome, and it helps them to escape from phagosome-lysosome fusion and spread to uninfected host cells by non-lytic ejection[18]. So far in this study we have correlated an increase in F-actin in Mtb-infected macrophages to reduced phagosome acidification. Now we propose a mechanism of action of ESAT-6 which might have resulted in the above observations.

In a recent study we have mentioned that downregulating reactive oxygen species (ROS) may drive the macrophages to a more anti-inflammatory phenotype[9]. A balanced inflammation is needed for the macrophage to efficiently contain the invading microbes[19]. It was reported that tuberculous granuloma contains more M2 macrophages (anti-inflammatory phenotype) than M1 macrophages (pro-inflammatory phenotype)[20] . We assume that secretory products of Mtb induce this anti-inflammatory effect. Also, ESAT-6 and CFP-10 were reported to downregulate ROS in macrophages[21].

To this end we hypothesize that a direct scavenging of ROS by ESAT-6 is possible and propose that the amino acid methionine in the exposed portions of the protein may react with superoxide/ROS to form methionine sulfoxide that in turn reduces the ROS concentration needed to drive effective pro-inflammatory signaling. Also, the cytoplasmic methionine sulfoxide reductase of macrophage may convert the methionine sulfoxide formed in ESAT-6 back to methionine and exposes it again to ROS. The antioxidant function of methionine is well described in the literature[22, 23] and it is more sensitive to ROS than cysteine in protecting active sites of various enzymes[24]. The disordered regions of Prion proteins which extend out of neuronal plasma membranes contain multiple number of methionine and they scavenge oxidants[25]. A study of the structure of ESAT-6.CFP10 complex shows that it doesn't have pore

forming, nucleic acid interacting and catalytic properties[26], which gives support to our assumption.

There are 3 methionines in ESAT-6 including the starting one. We selected M93 to be mutated for finding its effect on ROS resistance. M93 is present in the C-terminal flexible arm of ESAT-6 which does not contribute to the structure of the protein. At the same time mutations in C-terminal flexible arm including the mutation of methionine were reported to cause loss of virulence imparted by ESAT-6[27].

Methionine 93 was mutated to alanine or cysteine. ESAT-6, ESAT-6 M93A and ESAT-6 M93C expressing *E. coli* were treated with 400µM H_2O_2 in broth culture and incubated for 6hrs and ODs were measured in every hour. The OD of *E.coli* containing the control plasmid remained zero throughout the period. *E. coli* containing ESAT-6 had the highest OD at all time points followed by *E. coli* with ESAT-6 M93A and ESAT-6 M93C respectively (Fig. 11). Even though the mutation of methionine to cysteine was designed to rescue the antioxidant function imparted by the presence of sulfhydryl groups in both of the amino acids, the effect of M93C mutant was nearer to the control in the above experiment. This may be due to the formation of double sulfide bond between cysteines. There is no cysteine in ESAT-6 or CFP-10 and many of the secreted virulent proteins of different bacteria do not contain cysteine[28].

Further, we transfected ESAT-6 and its mutants in macrophages and measured ROS after 24h post PMA induction using DCFDA fluorescence as a readout by flow cytometry. The result was more similar to that from the *E.coli* experiment (Fig. 12). Even though the graphs for ESAT-6 and ESAT-6 M93A mutant look similar, the area of low fluorescence populations is more in the case of ESAT-6 (and also the high fluorescence population is less to some extent) compared to the mutant.

If ESAT-6 downregulates/scavenges ROS, it may drive an anti-inflammatory effect in macrophages as stated earlier. We have already shown the effect of various anti-inflammatory stimuli on the expression of cofilin1 and related proteins. Therefore WB was done to check for the same in ESAT-6 or its methionine 93 mutants- transfected macrophages. Cofilin1 expression was reduced, and pCofilin1, LimK1, pLimK1 and coronin expressions were increased in ESAT-6- transfected macrophages (Fig. 13). These effects were partially reversed in most of the cases in ESAT-6 M93A and M93C mutants-transfected macrophages. The level of pCofilin1 almost reverts to its level in control plasmid- transfected macrophages when ESAT-6- transfected macrophages were treated with 100µM H_2O_2.

We also checked the effect of transfection of ESAT-6 and the mutants on F-actin and phagosome acidification. We got more spindle shaped (M2 like) macrophages with highly enriched F-actin in ESAT-6 transfection (Fig. 14). Phagosome acidification was also found reduced in ESAT-6- transfected macrophages (Fig. 15). These effects were partially nullified in the case of ESAT-6 mutants-transfected macrophages. In this experiment rifampicin-treated

(10µg/ml in infection medium) H37Ra was used for infection to ensure that no protein from the bacterium interfered in the infection process.

Further, we did *in silico* modeling to check for any structural changes caused by the M93 mutation in ESAT-6 and no considerable change was visible (Fig. 16). Along with this, the interaction of cytoplasmic methionine sulfoxide reductase (MSR- B) of macrophage with ESAT-6 was predicted and it was shown that the C-terminal flexible arm of ESAT-6 can easily be fitted in to the active site of MSR-B.

Discussion

Our study is rooted on the differential expression of cofilin1 of macrophages in an *in vitro* infection experiment. We guess that the upregulation of phosphocofilin1 in macrophages by virulent *M. tuberculosis* leads to enrichment of filamentous actin which in turn leads to improper phagosome processing. Increased phagosome acidification in infected macrophages expressing constitutively active cofilin1 strongly supports this assumption. We also showed that sorafenib which activates cofilin1 resulted in increased killing of Mtb in infected macrophages, giving an implication on the potential use of this kinase inhibitor for a host modulation therapy against tuberculosis.

Since cofilin1 is positively regulated by ROS we wanted to determine whether there is any effect by the ROS downregulating secreted protein of Mtb, ESAT-6, on cofilin1 or not. We found that ESAT-6 downregulates cofilin1 and results in decreased phagosome acidification. ESAT-6 is a prominently secreted protein from the RD1 genomic region of Mtb and it is absent in vaccine strain BCG[29]. Also, a mutation in the PhoP regulator contributes to the impaired secretion of ESAT-6 and attenuation of the avirulent Mtb strain, H37Ra[30]. Our study proposes a mechanism for downregulation of ROS by ESAT-6. Even though we do not provide evidence for direct scavenging of ROS by methionines of ESAT-6, we could show that mutation of M93 methionine can abrogate ROS resistance imparted by the protein. The peculiar structural features of ESAT-6 lead us to the above assumption as mentioned earlier and we also suggest that the interactions of ESAT-6 with host cell receptors/proteins may happen by the virtue of methionine aromatic motif (methionine and an aromatic amino acid alternate in this motif) like sequence in the C-terminal arm since there is a phenylalanine near to M93[31].

The proposed mechanism of action of ESAT-6 on the antioxidant function wherein its multiple methionines contributing to its virulence lead us to speculate that similar mechanism may hold good in the case of ESAT-6 like proteins, for example, CFP-10. Since the Mtb genome contains many duplications of the Region of Difference (RD)[32] and most of the ESAT-6 like proteins, PE-PPE proteins and other hypothetical proteins which are secreted abundantly, but do not appear to have a role in the growth of the bacterium outside the host, a concerted action of all of these proteins may contribute to the virulence of the pathogen. The mechanism we proposed also

implicates the possible scavenging of ROS by different biomolecules like carotenoids and sugars like mannose in various pathogens, might be contributing to their virulence.

Materials and methods

Cell culture, bacteria and infection

THP1 monocytic cell line was maintained in RPMI-1640 medium (R4130, Sigma) supplemented with 10 % FBS. For obtaining macrophage monolayer THP1 cells with required cell density (3×10^6 cells in T-25 flask and 4×10^4 cells per well in a 96 well plate) were treated with 20ng/ml of PMA (P8139, Sigma) and after one day PMA was washed off 2 times with RPMI. After washing the cells 3ml and 100µl complete medium was maintained until the addition of bacteria in T-25 flask and 96 well plate respectively (for 96 well plate bacteria were added in a100µl suspension). Stocks of *Mycobacterium tuberculosis* strains, H37Rv and H37Ra were prepared using beads (PROTECT bacterial preservers) and stored at -80^0C. Periodically, the frozen stocks were revived in7H9 broth and streaked on LJ slants and maintained for at least 2 months in an incubator at 37^0C. Prior to experiments bacteria were inoculated into 7H9 broth (271310, Difco) from LJ slants. 7-10 days old broth cultures were used for infection experiments. An OD of 0.15 at 610 nm was measured to give McFarland standard 1 and was calculated to contain 3×10^8 bacteria/ml. On the day of infection log phase culture of bacteria was collected and passed through a syringe for 20 times and kept for 10 min to remove the clumps and the required volume of the culture was pelleted by centrifugation at 3000g for 10 min. Then the pellet was resuspended in RPMI and added to the macrophage monolayer. For increasing the infection efficiency, minimum volume of bacterial suspension was used to infect monolayer of macrophages. After the addition of bacteria the macrophage monolayer was kept for 4h for phagocytosis. After 4h the extracellular bacteria were washed off 3 times with RPMI and complete medium was added.

Chemicals

Chemicals and their respective concentrations used for the treatment of infected and uninfected macrophages are listed below. H_2O_2-100µM, NAC (A7250, Sigma) -10mM, PDTC (P8765, Sigma) -50µM, GÖ6983 (G1918, Sigma) -500nM, DPI (D2926, Sigma) - 10µM, LPS (L4391, Sigma) -1µg/ml, recombinant TNFα (RTNFAI, Thermo) -10ng/ml, Vitamin D- 100nM (C9756, Sigma) and Sorafenib -5 µM (SML2653**,** Sigma)

2D gel electrophoresis

After 24h of infection, total protein of infected and uninfected macrophages was isolated using 2D lysis buffer composed of 8M urea, 1M thiourea and 4% CHAPS along with 1mM PMSF. After 30 minutes of incubation at room temperature the cell lysate was centrifuged at 14000g for 20 min at 18^0C and then 300µg of total protein was loaded on a 7cm IPG strip of 3-10 pI range (163-2000, BIO RAD). After isoelectric focusing, the strips were equilibrated and

PAGE (15% gel) was run to resolve the proteins. From the gel, visually identified spot was picked and analyzed by MALDI-TOF-TOF.

Quantitative RT-PCR

After 12h of infection, total RNA of infected and uninfected macrophages was isolated using Illustra RNAspin (25-0500-71, GE) and the concentration was estimated by NanoVue Plus, GE. Primers for the genes were designed by Primer Premier Software. Primer pair for the reference gene GAPDH: FP: 5' TCAAGAAGGTGGTGAAGCA 3', RP: 5' AGGTGGAGGAGTGGGTGT 3'. Primer pair for cofilin: FP: 5'GCCTGAGTGAGGACAA3', RP: 5' GACAAAGGTGGCGTAG 3'.Primer efficiency for cofilin: 93.4% and GAPDH : 92.15%. qRT-PCR was performed using iScript one step RT-PCR kit (170-8892, BIO RAD). The relative quantitation and calculation of primer efficiency were done by the same software (CFX manager, BIO RAD) which performed the RT-PCR

Western blot

At various time points, infected and uninfected macrophage monolayers were washed with ice cold PBS, scraped in 1ml PBS and were centrifuged at 2000 rpm for 5 min at 4^0C. The cell pellet was lysed with RIPA buffer (R0278, Sigma) in the presence of protease inhibitor cocktail (P8340, Sigma). After 5min of incubation on ice, the cell lysate was centrifuged at 14000g for 10min at 4^0C and supernatant was collected. Protein was estimated using a BCA kit (23225, Thermo) and loaded at 15µg per well. β-tubulin (ab6046, abcam) was used as loading control. Blot was probed by anti-cofilin antibody (ab42824, abcam), anti-cofilin –phospho S3-antibody (ab131274, abcam), anti-LimK1 antibody (ab81046, abcam), anti-LimK1-phospho T508-antibody (ab131341, abcam) or anti-coronin 1a antibody (ab119094, abcam) and subsequently with anti-rabbit secondary antibody HRP (sc-2004, Santa Cruz) or anti-mouse secondary antibody (Sigma), and was developed using ECL Prime (RPN2232, GE) or using manually prepared luminol (Sigma). Relative expression was calculated by taking the ratio of intensities of respective proteins to that of β-tubulin using Quantity One or Image lab software (BIO RAD)

Confocal microscopy

THP1 cells were seeded in an optical bottom 96 well plate at 4×10^4 cells per well and induced to form macrophage monolayer. The cells were fixed by 4% paraformaldehyde, permeabilized by 0.1% Triton X100 and blocked with 3% BSA and 0.3M glycine in PBS. Images were taken under 40X objective with a confocal microscope (Nikon).

Phalloidine Red staining: After fixation and permeabilization of macrophage monolayers incubation of a working solution of the dye (Acti- stain 555,PHDH1, Cytoskeleton) in PBS at 100nM (stock-14µM in methanol) was done at room temperature in dark for 30min. Then, washed 3 times with PBS and imaged.

Lysotracker Red staining: a 100nM concentration of the dye (Invitrogen) was prepared in RPMI and incubated the cells for 40min in a CO_2 incubator. Then, washed 3 times with PBS and processed for imaging by confocal microscopy.

DCFDA fluorescence measurement by flow cytometry: Macrophages were seeded at 3 million/T-25 flask, washed 3 times with RPMI, detached the cells using a non-trypsin reagent (Sigma) and suspended the cells in RPMI containing 10µM DCFDA, incubated in CO_2 incubator for 30min, centrifuged, washed twice with PBS and analyzed by flow cytometry using 488nm laser.

Plating and colony count

To find out the effect of sorafenib treatment on the survival of bacteria, macrophages were infected with H37Rv. After 4h of phagocytosis gentamicin was added to the medium at 15µg/ml and incubated for 1h to kill the extracellular bacteria, then washed 3 times with RPMI. Sorafenib was treated after one day of infection, continued the treatment for another two days and after that the cells were lysed with sterile distilled water, diluted to 10^{-2} and plated on 7H10 agar (262710, Difco) supplemented with 0.1% casitone (0259-17, Difco). Colonies were counted after 3 weeks.

Ectopic expression of ESAT-6 in macrophages

ESAT-6 was amplified from H37Rv DNA using the following primers; FP: 5' CGGAATTCCGATGACAGAGCAGCAGTGGAAT3' with EcoR1 site and RP: 5'CGACGCGTCGCTATGCGAACATCCCAGTGACG3' with Mlu1 site. The amplified fragment was cloned into MCS A of pIRES (Clontech). The reporter gene ECFP was taken from pECFP-N1 (Clontech) by restriction digestion at Sal1 and Not1 sites and ligated into MCS B of pIRES. The insertions were confirmed by both restriction digestion and sequencing. The plasmid was isolated using an endotoxin free plasmid isolation kit (EndoFree Plasmid Maxi Kit, Cat. No. 12362, QIAGEN). Before transfection THP1 cells were washed in serum free RPMI for 2 times. Then a 10-20 µg of plasmid was mixed with 40×10^6 THP1 monocytes suspended in serum free RPMI in a 4mm electroporation cuvette and electroporated at the given conditions; choose mode-LV, pulse length-5ms, charging voltage-350V in a BTX Harvard Apparatus, ECM 830. Cells were incubated for 10min on ice before and after electroporation and transferred to culture flasks containing RPMI+10%FBS and incubated for 24hrs. After 24hrs the viable cells were counted using Trypan blue (T8154, Sigma) staining, seeded into plates at respective densities and treated with PMA for next 24hrs.For Western blot a 10µg of total protein was loaded. Transfection of cells was confirmed by imaging the cells with 405nm laser for ECFP expression with a confocal microscope

Creation of ESAT-6 M93 mutants: M93A and M93C mutants of ESAT-6 were made by manually changing the codon for methionine to alanine or cysteine in the reverse primer of ESAT-6 gene and cloning was done as described earlier.

E. coli containing pIRES plasmid with ESAT-6 or its mutants were used to check ROS resistance since the immediate early CMV promoter in the plasmid is active in the bacteria also[33].

F-actin/G-actin ratio

F-actin stabilization buffer: 0.1M PIPES at pH-6.9, 30% glycerol, 5% DMSO, 1mM $MgSO_4$, 1mM EGTA, 1% IgePal and 1mM ATP

F-actin depolymerization buffer: 0.1M PIPES at pH-6.9, 1mM $MgSO_4$, 10mM $CaCl_2$ and 8M urea.

The cells were lysed with actin stabilization buffer on ice for 10min and centrifuged at 4^0C for 75min at 16000g. Supernatant was collected, containing the G-actin portion. The pellet containing F-actin was solubilized in the depolymerization buffer. Both the F-actin and G-actin portions were loaded at 10µl each with loading dye. The Western blot was probed with an anti-β-actin antibody (Sigma).

MTT assay

MTT reagent (M2128, Sigma) was dissolved in PBS at 5mg/ml. 20µl of MTT solution was added to 200µl of culture medium of infected macrophages in each well of a 96 well plate and incubated for 4h. After the incubation the solution was aspirated and 100µl of DMSO was added to each well. The content was mixed by keeping the plate on a rocker for 5 min and absorbance was measured at 570 nm. Background absorbance was measured at 690 nm and subtracted from the value at 570 nm.

Statistical analysis

Statistical analysis was done using IBM SPSS statistics software, version 19. Comparison of means was done by one way ANOVA (Tukey's method) by setting alpha value as 0.05. Values were expressed as mean ± SE.

References

1. Cambier, C.J., Falkow, S., and Ramakrishnan, L. (2014). Host Evasion and Exploitation Schemes of Mycobacterium tuberculosis. Cell *159*, 1497–1509.
2. Liebl, D., and Griffiths, G. (2009). Transient assembly of F-actin by phagosomes delays phagosome fusion with lysosomes in cargo-overloaded macrophages. J. Cell Sci. *122*, 2935–2945.
3. Kolonko, M., Geffken, A.C., Blumer, T., Hagens, K., Schaible, U.E., and Hagedorn, M. (2014). WASH-driven actin polymerization is required for efficient mycobacterial phagosome maturation arrest. Cell. Microbiol. *16*, 232–246.

4. Bernstein, B.W., and Bamburg, J.R. (2010). ADF/Cofilin: A functional node in cell biology. Trends Cell Biol. *20*, 187–195.
5. Kanellos, G., and Frame, M.C. (2016). Cellular functions of the ADF/cofilin family at a glance. J. Cell Sci. jcs.187849.
6. Drengk, A., Fritsch, J., Schmauch, C., Rühling, H., and Maniak, M. (2003). A Coat of Filamentous Actin Prevents Clustering of Late-Endosomal Vacuoles in Vivo. Curr. Biol. *13*, 1814–1819.
7. Moon, A., and Drubin, D.G. (1995). The ADF/cofilin proteins: stimulus-responsive modulators of actin dynamics. Mol. Biol. Cell *6*, 1423–1431.
8. Taulet, N., Delorme-Walker, V.D., and DerMardirossian, C. (2012). Reactive Oxygen species regulate protrusion efficiency by controlling actin dynamics. PLoS One *7*.
9. Mahesh, P.P., Retnakumar, R.J., and Mundayoor, S. (2016). Downregulation of vimentin in macrophages infected with live Mycobacterium tuberculosis is mediated by Reactive Oxygen Species. Sci. Rep. *6*, 21526.
10. Gandhi, M., Achard, V., Blanchoin, L., and Goode, B.L. (2009). Coronin Switches Roles in Actin Disassembly Depending on the Nucleotide State of Actin. Mol. Cell *34*, 364–374.
11. Galkin, V.E., Orlova, A., Brieher, W., Kueh, H.Y., Mitchison, T.J., and Egelman, E.H. (2008). Coronin-1A Stabilizes F-Actin by Bridging Adjacent Actin Protomers and Stapling Opposite Strands of the Actin Filament. J. Mol. Biol. *376*, 607–613.
12. Ferrari, G., Langen, H., Naito, M., and Pieters, J. (1999). A coat protein on phago- somes involved in the intracellular survival of mycobacteria. Cell *97*, 435–447.
13. Hart, B.Y.P.D.A., Young, M.R., Gordon, A.H.,and Sullivan, K.H. (1987). INHIBITION OF LYSOSOMAL MOVEMENTS OBSERVED AFTER PHAGOCYTOSIS MACROPHAGES BY CERTAIN MYCOBACTERIA CAN BE EXPLAINED BY INHIBITION OF PHAGOSOME-LYSOSOME FUSION IN CULTURED MACRO- PHAGES OR MONOCYTES. J. Exp. MED *166*.
14. Wang, Z., Wang, M., and Carr, B.I. (2010). Involvement of receptor tyrosine phosphatase DEP-1 mediated PI3K-cofilin signaling pathway in Sorafenib-induced cytoskeletal rearrangement in hepatoma cells. J. Cell. Physiol. *224*, 559–565.

15. Garvalov, B.K., Flynn, K.C., Neukirchen, D., Meyn, L., Teusch, N., Wu, X., Brakebusch, C., Bamburg, J.R., and Bradke, F. (2007). Cdc42 regulates cofilin during the establishment of neuronal polarity. J. Neurosci. *27*, 13117–13129.
16. Ferreira, G.B., Baeke, F., De Clercq, V.P., Waelkens and Overbergh, M.L.(2013). A proteomic approach on the effects of TX527, a 1,25-dihydroxyvitamin D3 analog, in human T lymphocytes. J. Steroid Biochem. Mol. Biol. http://dx.doi.org/10.1016/j.jsbmb.
17. MacGurn, J.A., and Cox, J.S. (2007). A genetic screen for Mycobacterium tuberculosis mutants defective for phagosome maturation arrest identifies components of the ESX-1 secretion system. Infect. Immun. *75*, 2668–2678.
18. Hagedorn, M., Rohde, K.H., Russell, D.G., and Soldati, T. (2009). Infection by tubercular mycobacteria is spread by nonlytic ejection from their amoeba hosts. Science *323*, 1729–1733.
19. Dorhoi, A., and Kaufmann, S.H.E. (2014). Perspectives on host adaptation in response to Mycobacterium tuberculosis: Modulation of inflammation. Semin. Immunol. *26*, 533–542.
20. Marino, S., Cilfone, N. a., Mattila, J.T., Linderman, J.J., Flynn, J.L., and Kirschner, D.E. (2015). Macrophage Polarization Drives Granuloma Outcome during Mycobacterium tuberculosis Infection. Infect. Immun. *83*, 324–338.
21. Ganguly, N., Giang, P.H., Gupta, C., Basu, S.K., Siddiqui, I., Salunke, D.M., and Sharma, P. (2008). Mycobacterium tuberculosis secretory proteins CFP-10, ESAT-6 and the CFP10:ESAT6 complex inhibit lipopolysaccharide-induced NF-kappaB transactivation by downregulation of reactive oxidative species (ROS) production. Immunol. Cell Biol. *86*, 98–106.
22. Luo, S., and Levine, R.L. (2009). Methionine in proteins defends against oxidative stress. FASEB J. *23*, 464–472.
23. Levine, R.L., Mosoni, L., Berlett, B.S., and Stadtman, E.R. (1996). Methionine residues as endogenous antioxidants in proteins. Proc. Natl. Acad. Sci. U. S. A. *93*, 15036–15040.
24. Estell, D.A., Graycar, T.P., and Wells, J.A. (1985). Engineering an Enzyme by Site-directed Mutagenesis to Be Resistant to Chemical Oxidation. Enzyme. 6518–6521
25. Requena, J.R., Dimitrova, M.N., Legname, G., Teijeira, S., Prusiner, S.B., and Levine, R.L. (2004). Oxidation of methionine residues in the prion protein by hydrogen peroxide. Arch. Biochem. Biophys. *432*, 188–195.

26. Renshaw, P.S., Lightbody, K.L., Veverka, V., Muskett, F.W., Kelly, G., Frenkiel, T.A., Gordon, S. V., Hewinson, R.G., Burke, B., Norman, J., et al. (2005). Structure and function of the complex formed by the tuberculosis virulence factors CFP-10 and ESAT-6. EMBO J. *24*, 2491–2498.
27. Brodin, P., De Jonge, M.I., Majlessi, L., Leclerc, C., Nilges, M., Cole, S.T., and Brosch, R. (2005). Functional analysis of early secreted antigenic target-6, the dominant T-cell antigen of Mycobacterium tuberculosis, reveals key residues involved in secretion, complex formation, virulence, and immunogenicity. J. Biol. Chem. *280*, 33953–33959.
28. Mejia, J.S., Arthun, E.N., and Titus, R.G. (2010). Cysteine-free proteins in the immunobiology of arthropod-borne diseases. J. Biomed. Biotechnol. *2010*.
29. Lewis, K.N., Liao, R., Guinn, K.M., Hickey, M.J., Smith, S., Behr, M.A., and Sherman, D.R. (2003). Deletion of RD1 from Mycobacterium tuberculosis Mimics Bacille Calmette-Guérin Attenuation . J. Infect. Dis. *187*, 117–123.
30. Frigui, W., Bottai, D., Majlessi, L., Monot, M., Josselin, E., Brodin, P., Garnier, T., Gicquel, B., Martin, C., Leclerc, C., et al. (2008). Control of M. tuberculosis ESAT-6 secretion and specific T cell recognition by PhoP. PLoS Pathog. *4*.
31. Valley, C.C., Cembran, A., Perlmutter, J.D., Lewis, A.K., Labello, N.P., Gao, J., and Sachs, J.N. (2012). The methionine-aromatic motif plays a unique role in stabilizing protein structure. J. Biol. Chem. *287*, 34979–34991.
32. Brosch, R., Gordon, S. V, Pym, a, Eiglmeier, K., Garnier, T., and Cole, S.T. (2000). Comparative genomics of the mycobacteria. Int. J. Med. Microbiol. *290*, 143–152.
33. Lewin, A., Mayer, M., Chusainow, J., Jacob, D., and Appel, B. (2005). Viral promoters can initiate expression of toxin genes introduced into Escherichia coli. BMC Biotechnol. *5*, 19.

Acknowledgements

This work was supported by intramural fund from RGCB. PPM was supported by a fellowship from Council for Scientific and Industrial Research, Govt of India. The authors thank Dr. Ajay Kumar, Dr. Jackson James, Dr. Omkumar, Dr. V.V Asha and Dr. Suparna Sen Gupta for providing some of the reagents.

Author Contribution statement:

PPM and SM designed the study and PPM performed the research work, and both wrote the manuscript together. RJR constructed plasmids, created ESAT-6 mutants and performed some of the experiments. SKC did the *in silico* modelling of ESAT-6 mutants.

Competing interests

The authors have declared that no competing interests exist.

Figure legends

Figure 1. *M. tuberculosis* downregulates cofilin1. a) 2DE images showing the spot for cofilin in different infection conditions. b) RT-PCR showing differential expression of cofilin gene at 12h post infection. c) Differential expression of cofilin and pCofilin in different infection conditions at 24h post infection. d) Differential phosphorylation of cofilin at zero hour (4h after addition of bacteria to macrophages) in different infection conditions. In all the cases, values are expressed as mean±SE. n=3. *Mean difference is significant at 0.05 level.

Figure 2. Differential expression of LimK1, pLimK1 and coronin in different infection conditions 24h post infection. Values are expressed as mean±SE. n=3. *Mean difference is significant at 0.05 level.

Figure 3. F-actin content of macrophages is increased on virulent Mtb infection. a) F-actin/G-actin ratios in different infection conditions. b) Phalloidine red staining of Mtb (GFP expressing)-infected macrophages. Images are representatives of three independent experiments.

Figure 4. Phagosome acidification (probed by Lysotracker Red) is less in virulent Mtb-infected macrophages.Images are representatives of three independent experiments

Figure 5. Sorafenib treatment reduces the F-actin content of Mtb-infected macrophages and PI3K inhibitor wortmannin reverses the effect of sorafenib. Images are representatives of three independent experiments

Figure 6. Sorafenib treatment increases phagosome acidification of virulent *M.tuberculosis*-infected macrophages and PI3K inhibitor wortmannin reverses the effect of sorafenib. Images are representatives of three independent experiments

Figure 7. Sorafenib treatment of infected macrophages kills *M.tuberculosis*. a) Colonies of H37Rv from infected macrophages with or without sorafenib treatment. Plated after

diluting to 10^{-2}. N=10, p=0.003. b) MTT assay of macrophages treated with 1µM and 5µM sorafenib. N=6, p<0.05. Cell viability in all cases was compared to uninfected macrophages.

Figure 8. Transfection of S3A mutant of cofilin1 decreases F-actin content and increases phagosome acidification virulent *M.tuberculosis* -infected macrophages. a) Phalloidine red staining of H37Rv-infected macrophages overexpressing constitutively active cofilin. b) Lysotracker Red staining of H37Rv-infected macrophages overexpressing constitutively active cofilin. c) Spreading of blue color in transfected macrophages shows the ECFP expression compared to non-transfected macrophages with the blue color confined to nucleus alone, when DAPI-treated macrophages were imaged with a 405nm laser. Images are representatives of three independent experiments.

Figure 9. Cofilin1 is activated by pro-inflammatory stimuli. Expression of cofilin1, LimK1, pLimK1 and coronin after 24h post infection, treated with different pro-inflammatory agents (Concentrations used: LPS-1µg/ml,H_2O_2-100µM, TNFα-10ng/ml, sorafenib-5 µM, vitamin D-100nM). Values are expressed as mean±SE, n=3. *Mean difference is significant at 0.05 level

Figure 10. Cofilin1 is inactivated by anti-inflammatory stimuli. Expression of cofilin1 and pCofilin1 a), LimK1 and pLimK1 b) and coronin c) after 24h post infection, treated with different anti-inflammatory agents.(Concentrations used: DPI -10µM,NAC -10mM, PDTC - 50µM). Values are expressed as mean±SE, n=3. *Mean difference is significant at 0.05 level

Figure 11. ESAT-6 makes *E.coli* resistant to hydrogen peroxide treatment. ESAT-6 and its mutants expressing *E. coli* were grown in broth culture and treated with 400µM H_2O_2 and ODs were measured.

Figure 12. ESAT-6 downregulates ROS and M93 mutation partially reverses this effect in transfected macrophages 24h post PMA induction. The images are representatives of 3 independent experiments.

Figure 13. ESAT-6 inactivates cofilin1 and this effect is partially reversed by its M93 mutation in transfected macrophages. Expression of cofilin1, LimK1, pLimK1 and coronin in macrophages transfected with ESAT-6 and its mutants 24h post PMA induction. Values are expressed as mean±SE, n=3. *Mean difference is significant at 0.05 level

Figure 14. ESAT-6 increases the F-actin content and transforms the macrophages to spindle shaped, and these effects are partially reversed by its mutants. Phalloidine red staining was used to visualize F-actin in H37Ra (GFP expressing, green) - infected macrophages expressing ESAT-6 or its mutants, 24h post infection. The images are representatives of 3 independent experiments.

Figure 15. ESAT-6 reduces phagosome acidification in avirulent H37Ra-infected macrophages and this effect was partially reversed by its mutants. Lysotracker Red staining was used to probe phagosome acidification in H37Ra (GFP expressing, green) - infected macrophages expressing ESAT-6 or its mutants, 24h post infection. The images are representatives of 3 independent experiments.

Figure 16. *In silico* modeling predicts that M93 mutations do not affect the structure of ESAT-6 considerably and the C-terminal flexible arm of ESAT-6 fits properly into the active site of methionine sulfoxide reductase. a) ESAT-6 and ESAT-6 M93A mutant interact with MSR-B. b) ESAT-6 and ESAT-6 M93C mutant interacts with MSR-B. (blue=ESAT-6, pink=ESAT-6 mutant and green=MSR-B).

Fig. 1

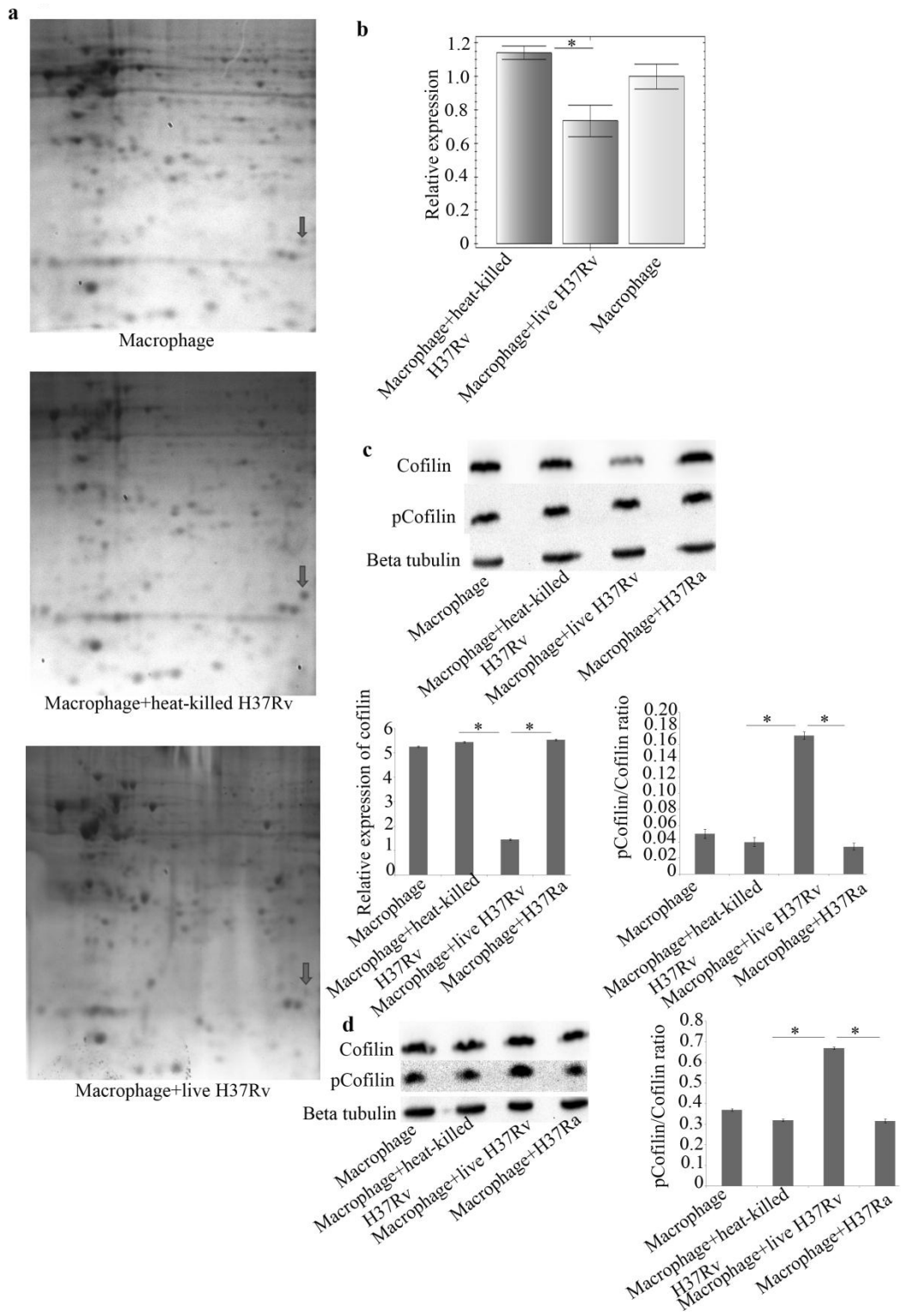

Fig. 2

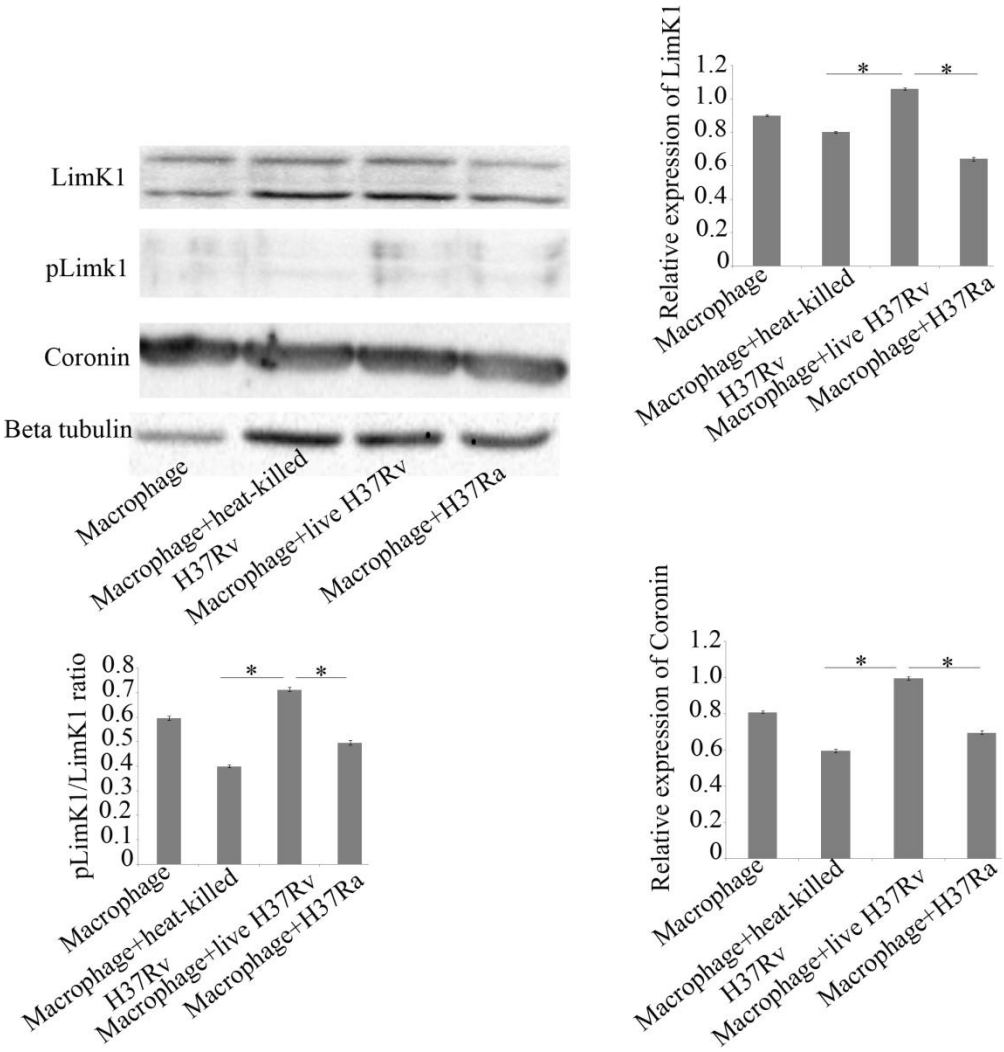

Fig. 3

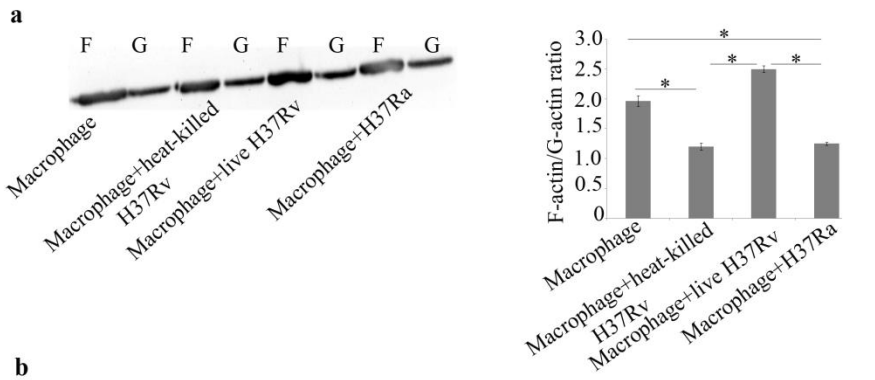

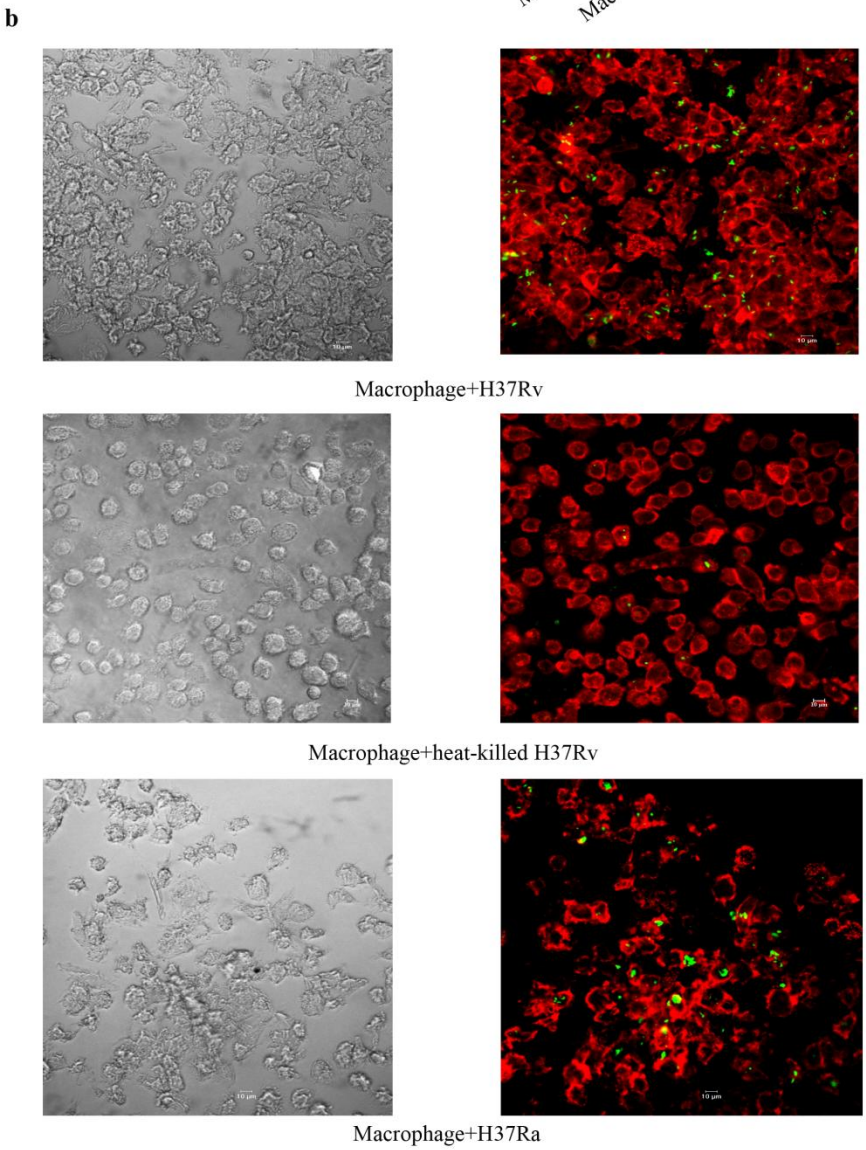

Fig. 4

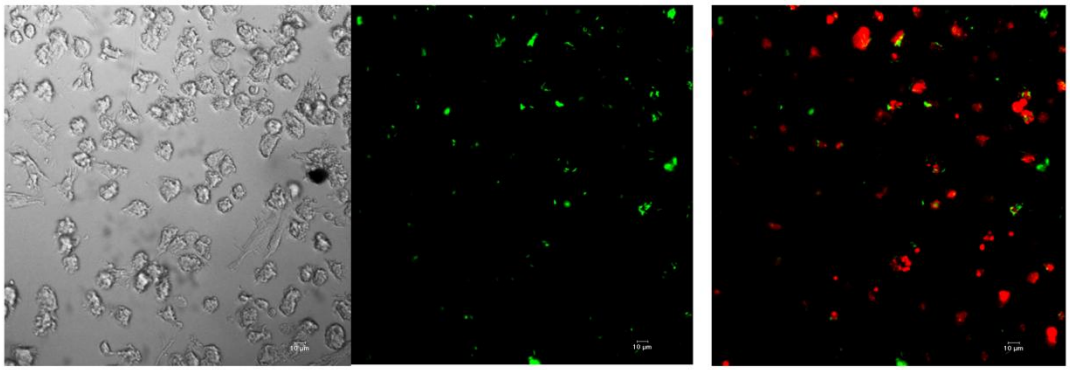

Macrophage+H37Rv

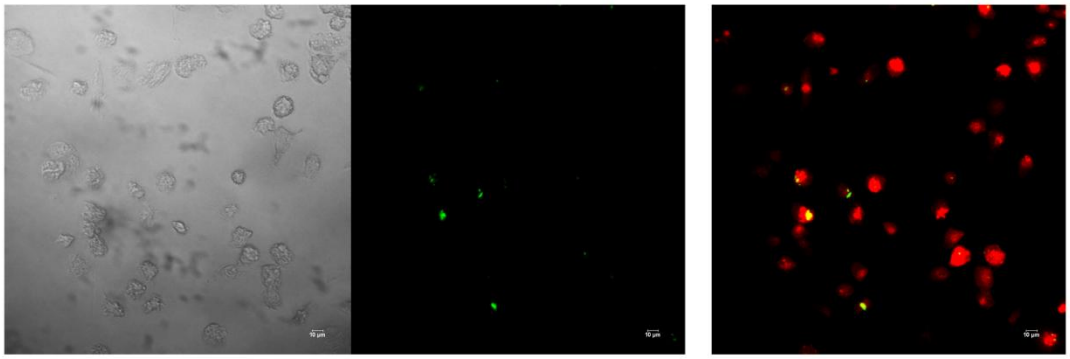

Macrophage+heat-killed H37Rv

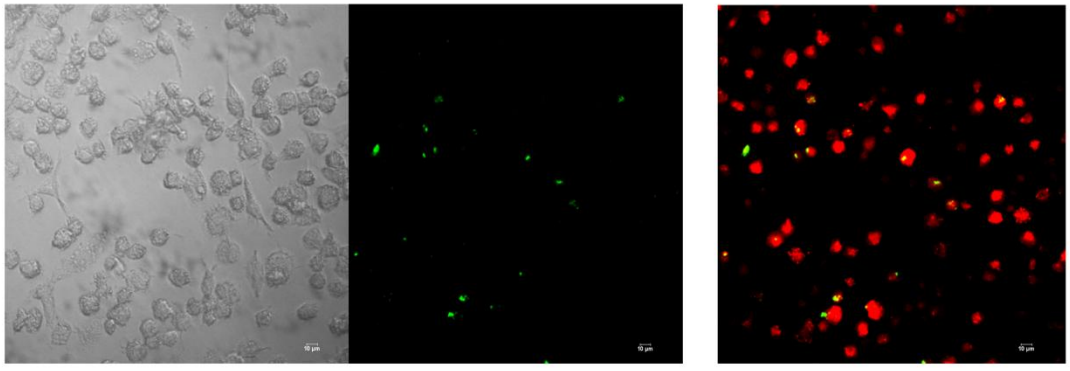

Macrophage+H37Ra

Fig. 5

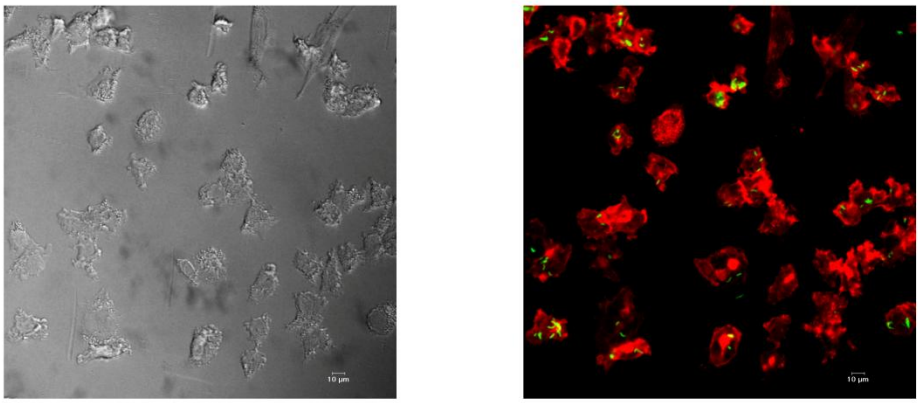

Macrophage+H37Rv

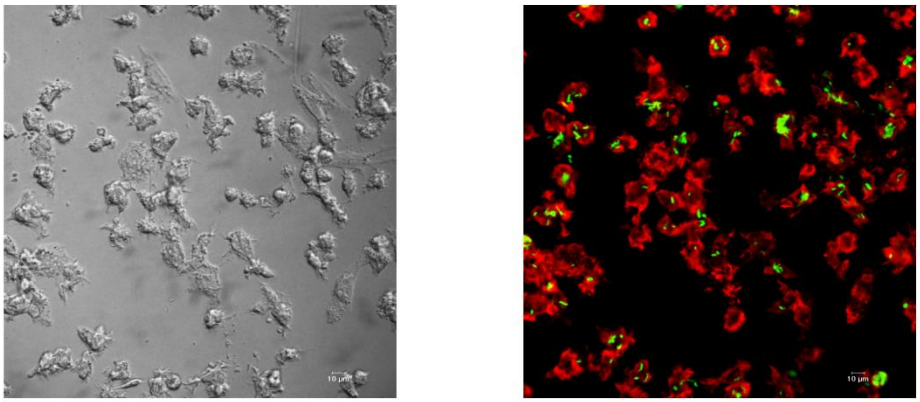

Macrophage+H37Rv+5μM sorafenib

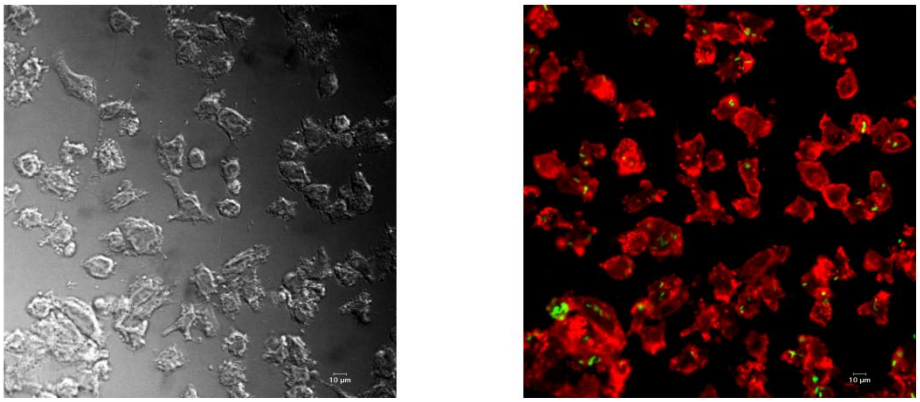

Macrophage+H37Rv+100nM wortmannin+5μM sorafenib

Fig. 6

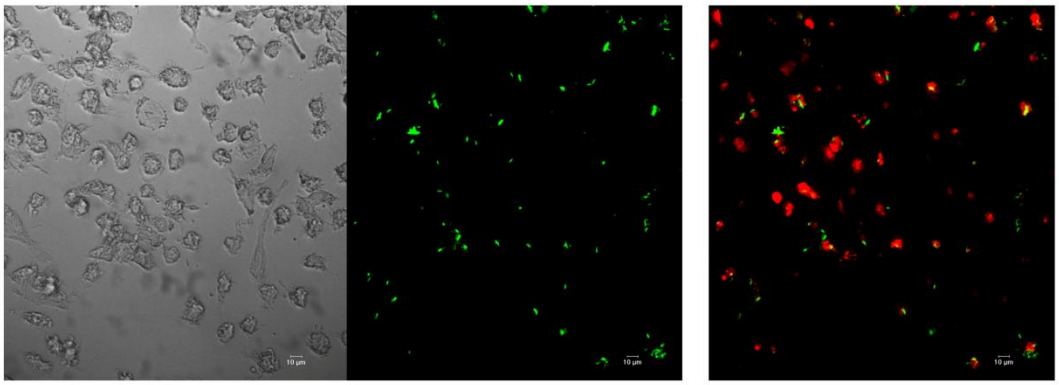

Macrophage+H37Rv

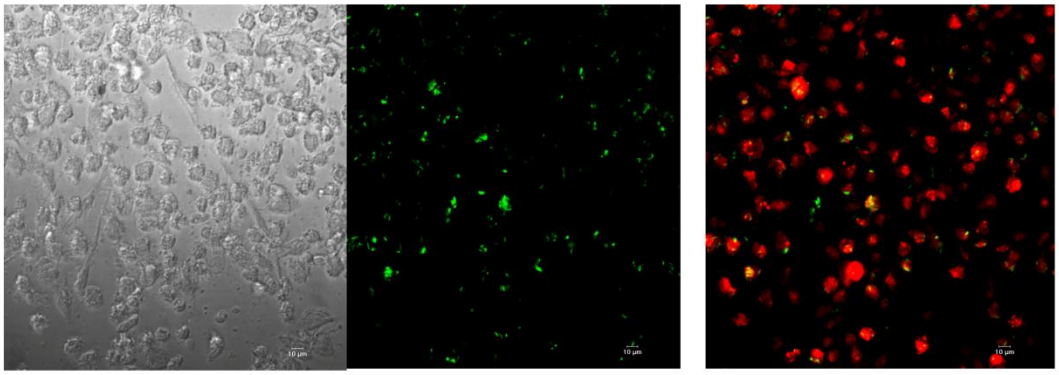

Macrophage+H37Rv+5μM sorafenib

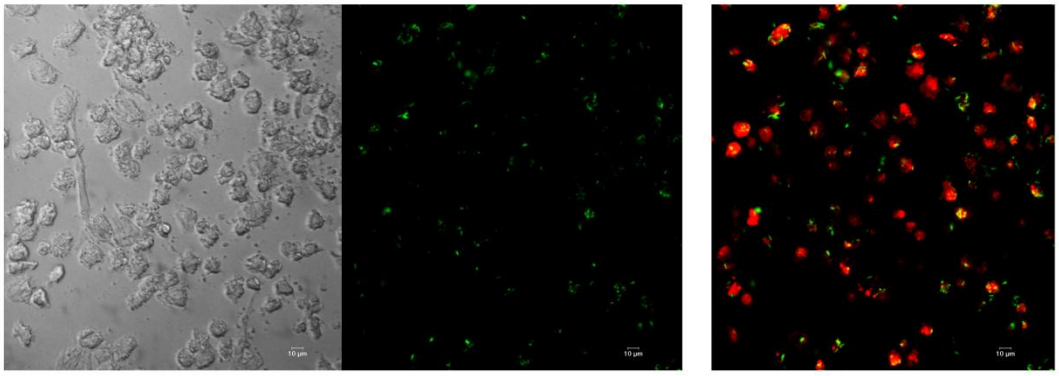

Macrophage+H37Rv+100nM wortmannin+5μM sorafenib

Fig. 7

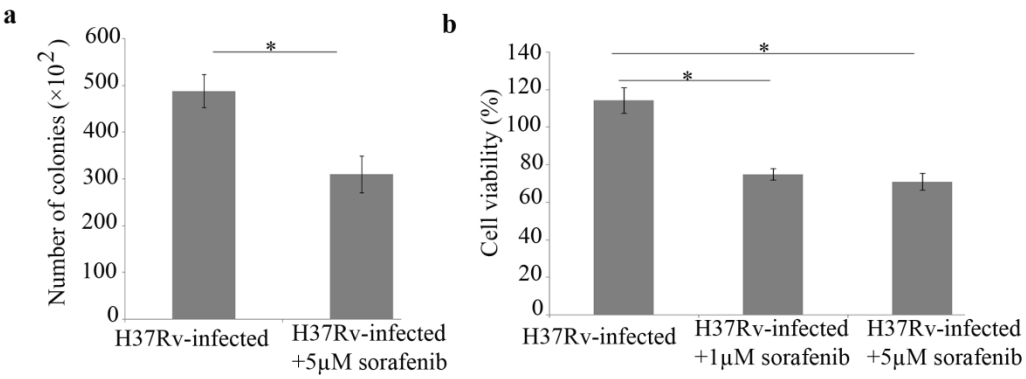

Fig. 8

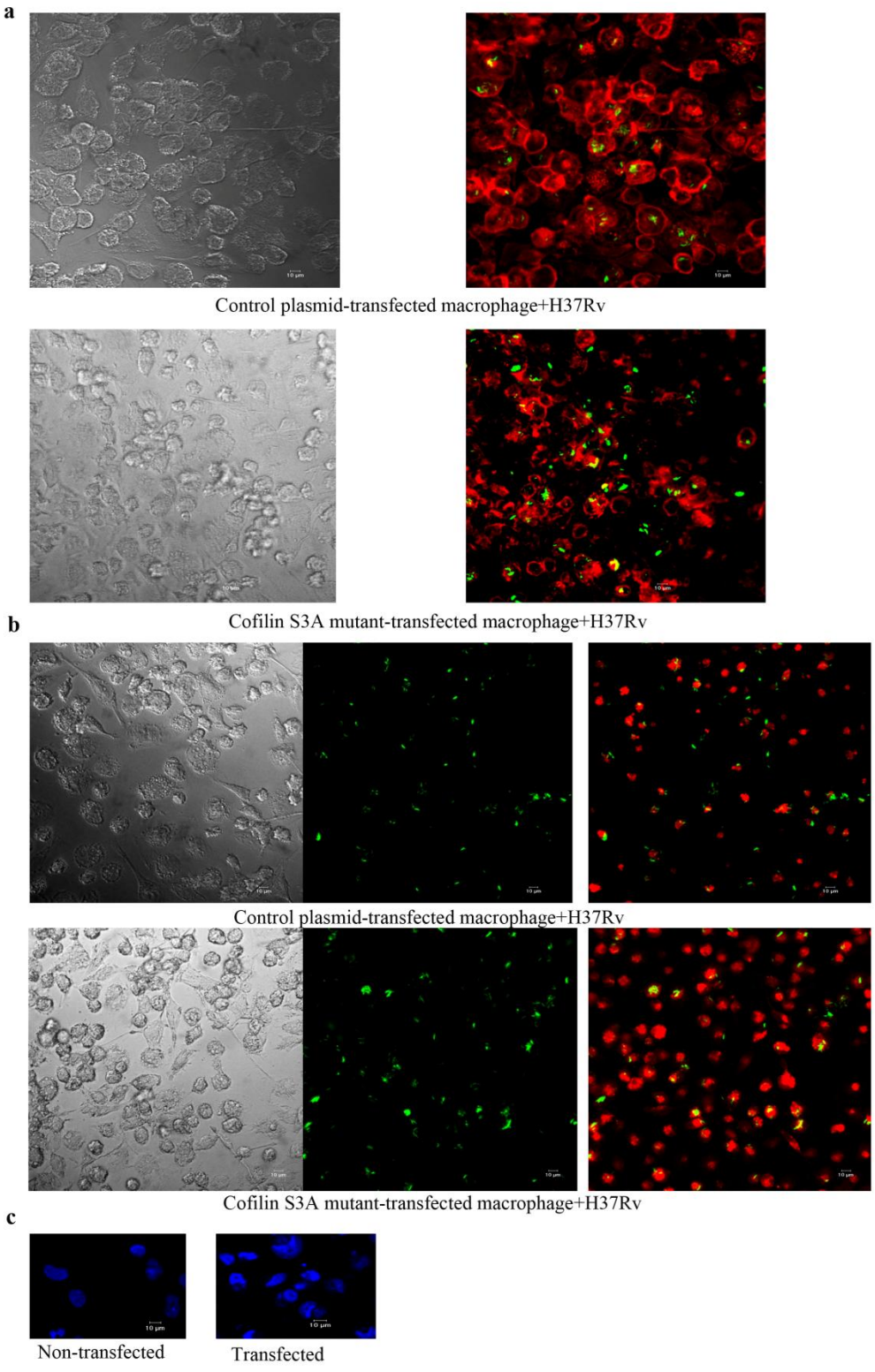

Fig. 9

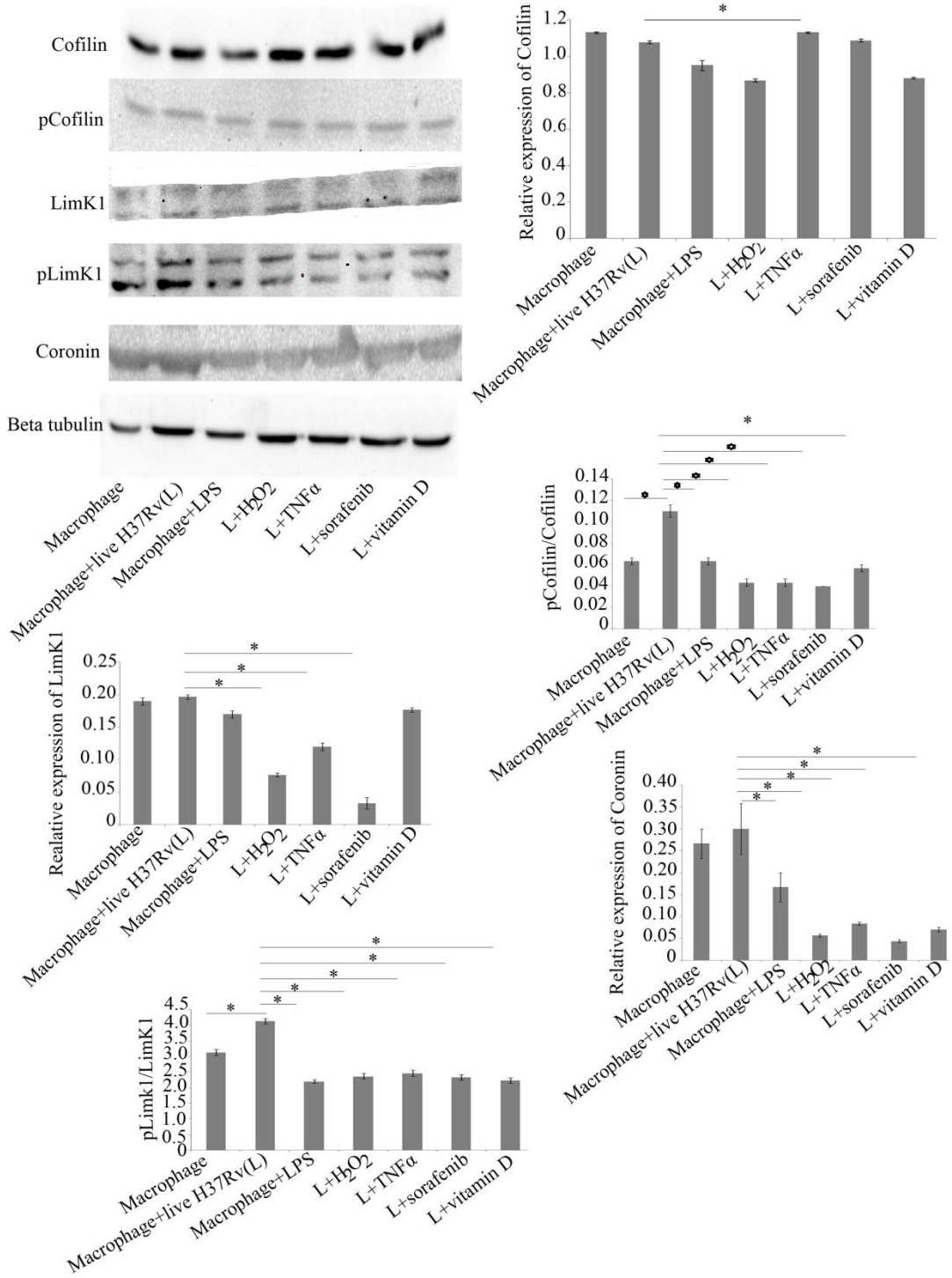

Fig. 10

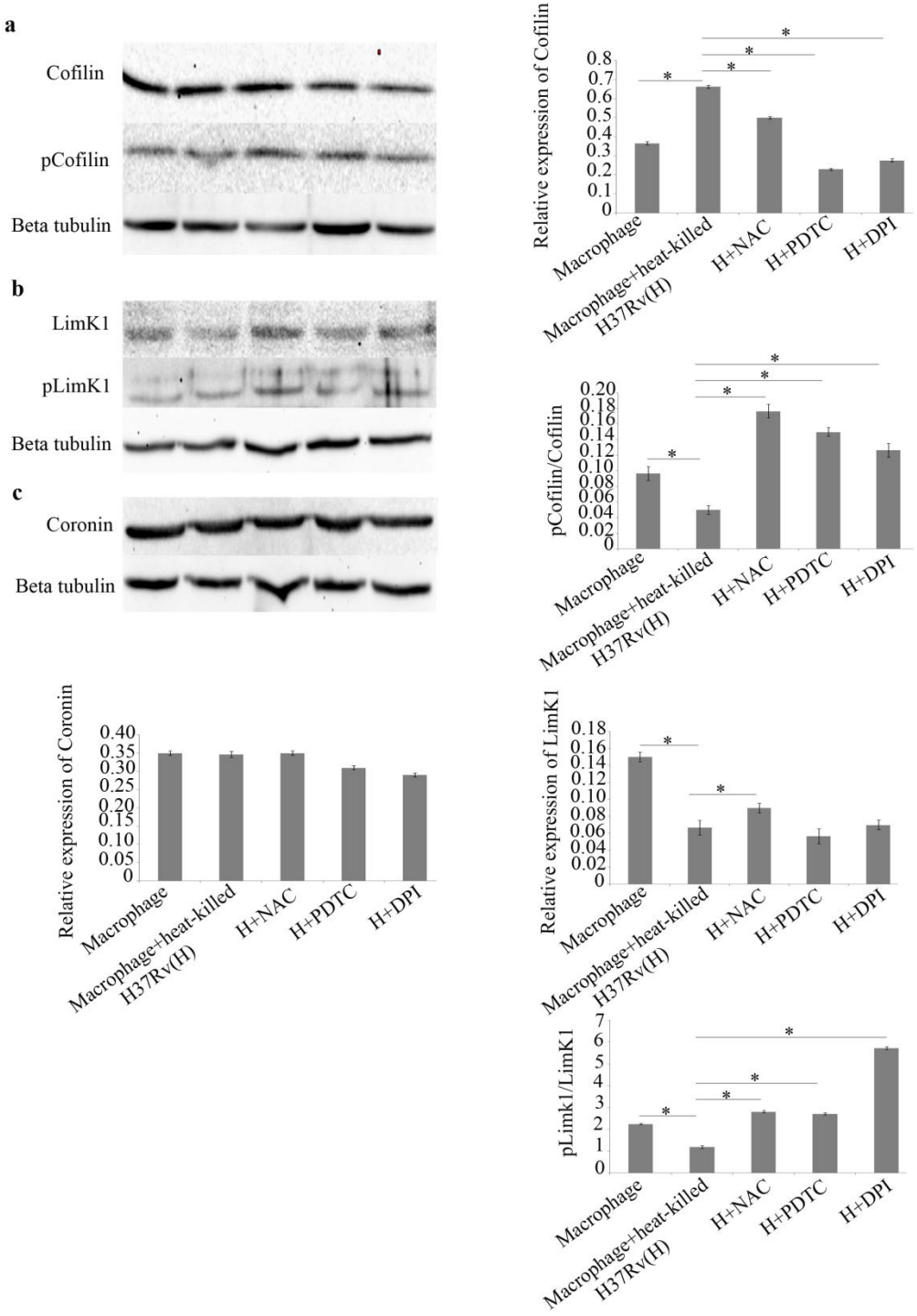

Fig. 11

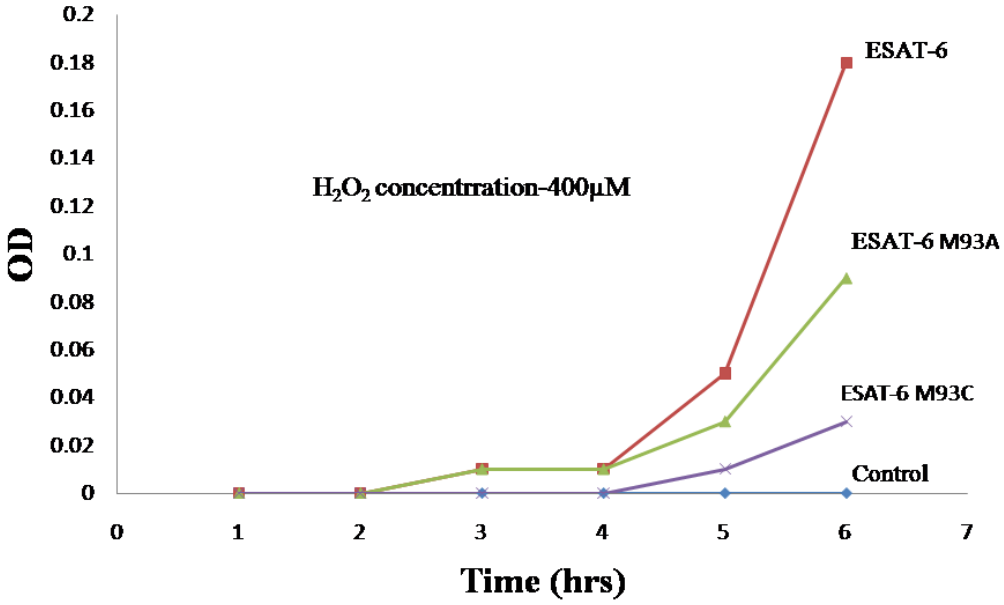

Fig. 12

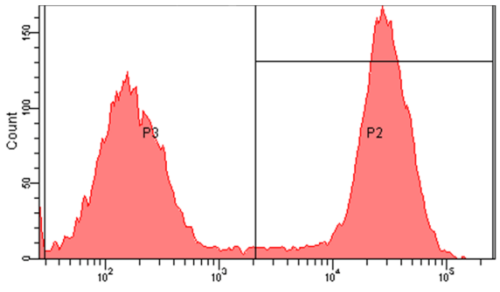

Macrophage+control plasmid

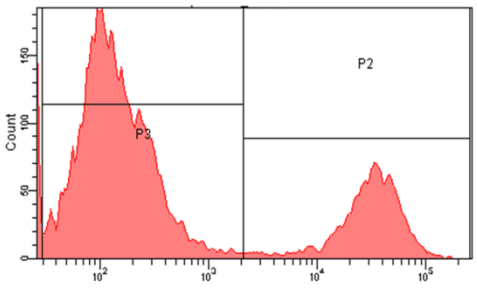

Macrophage+ESAT-6

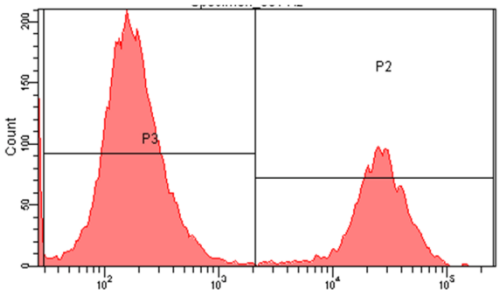

Macrophage+ESAT-6 M93A

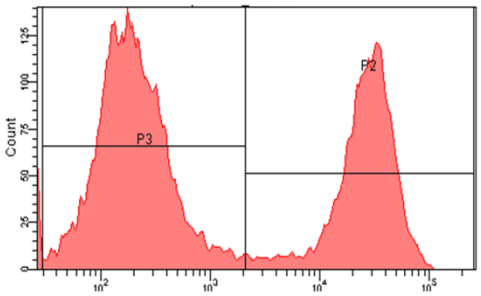

Macrophage+ESAT-6 M93C

Fig. 13

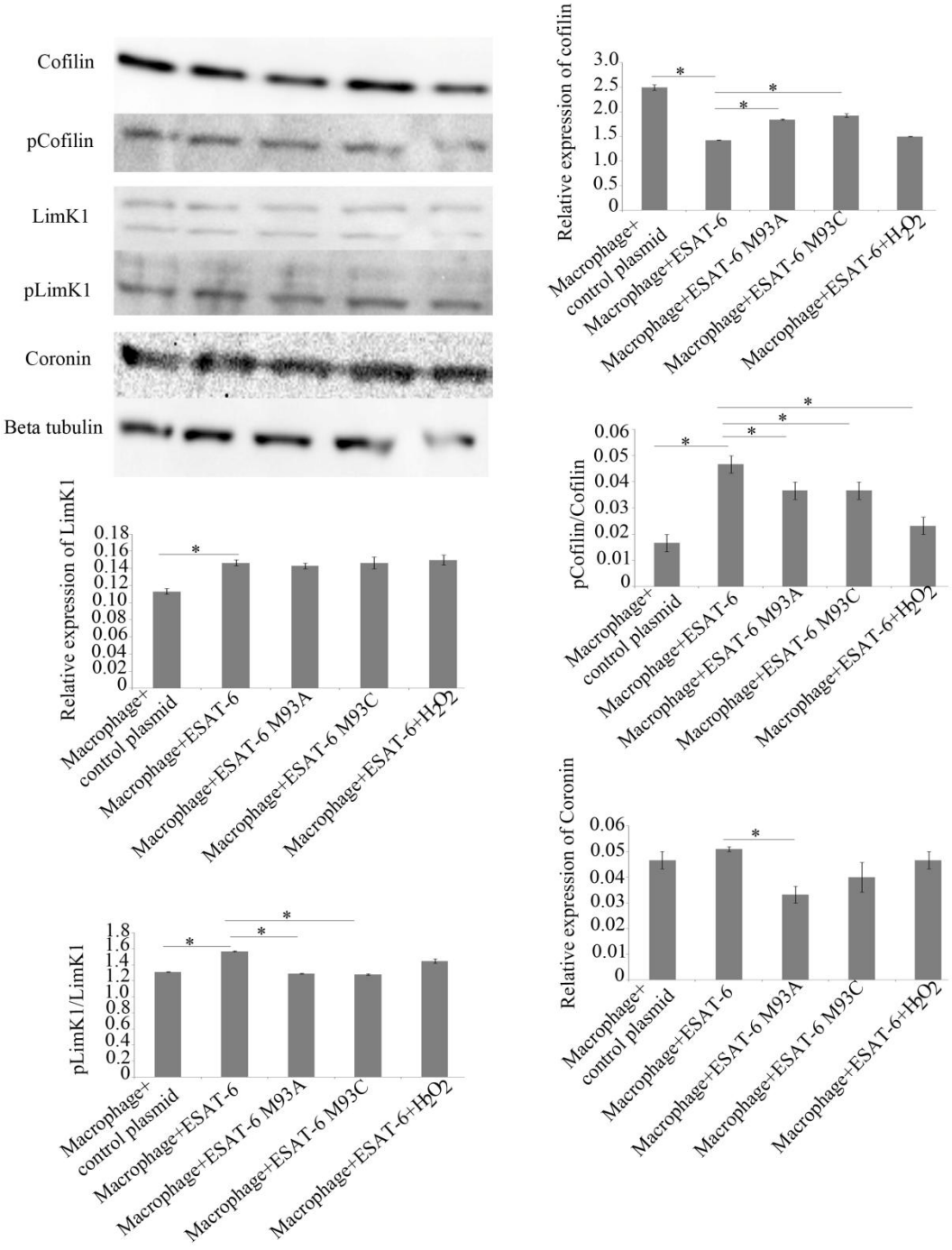

Fig. 14

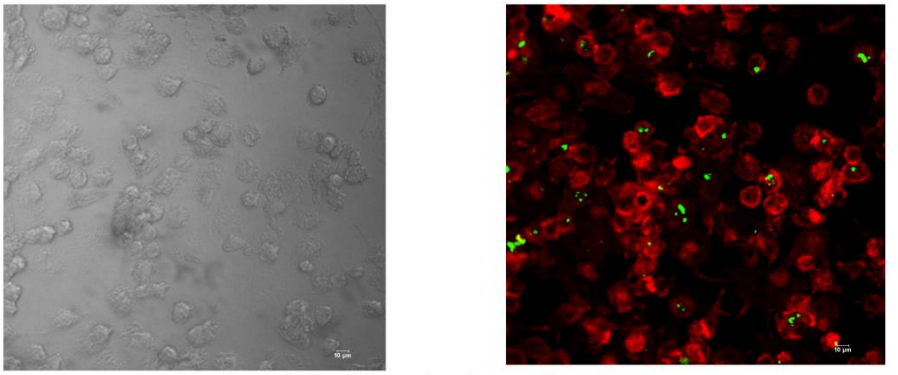

Control plasmid-transfected macrophage+H37Ra

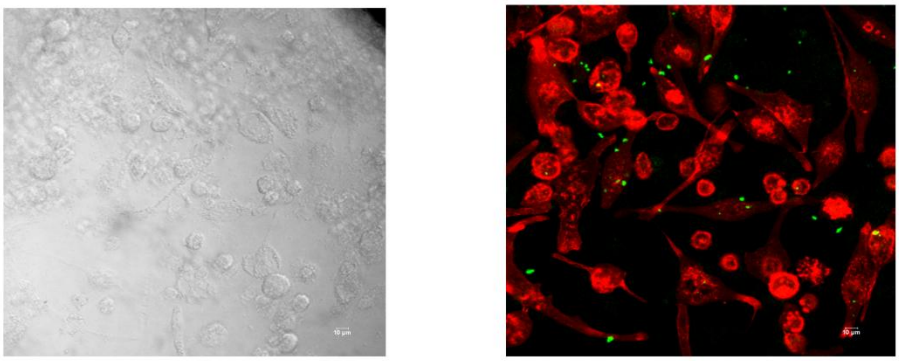

ESAT-6-transfected macrophage+H37Ra

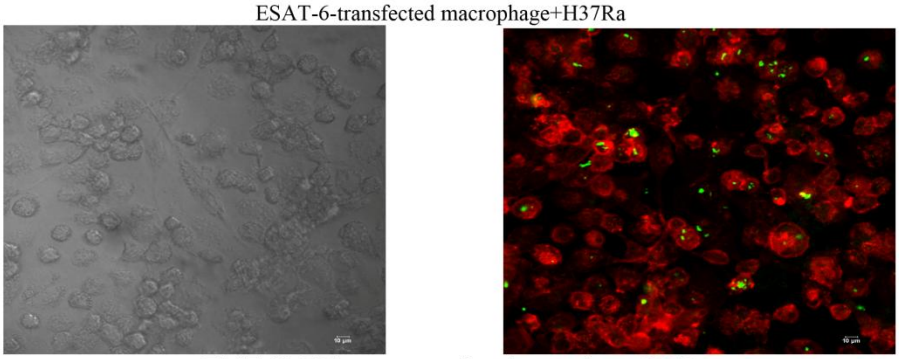

ESAT-6 M93A mutant-transfected macrophage+H37Ra

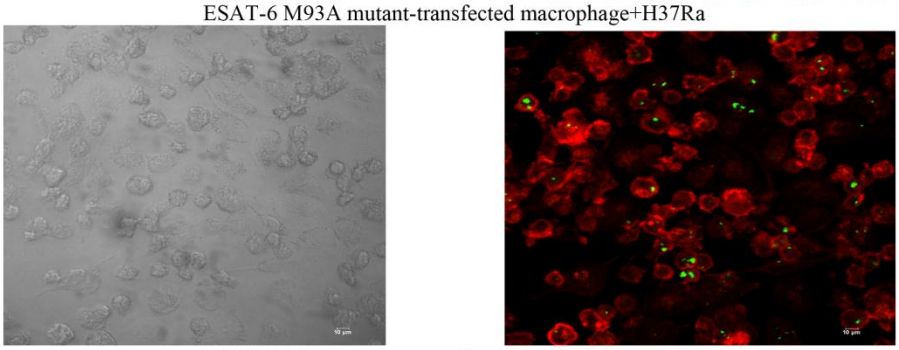

ESAT-6 M93C mutant-transfected macrophage+H37Ra

Fig. 15

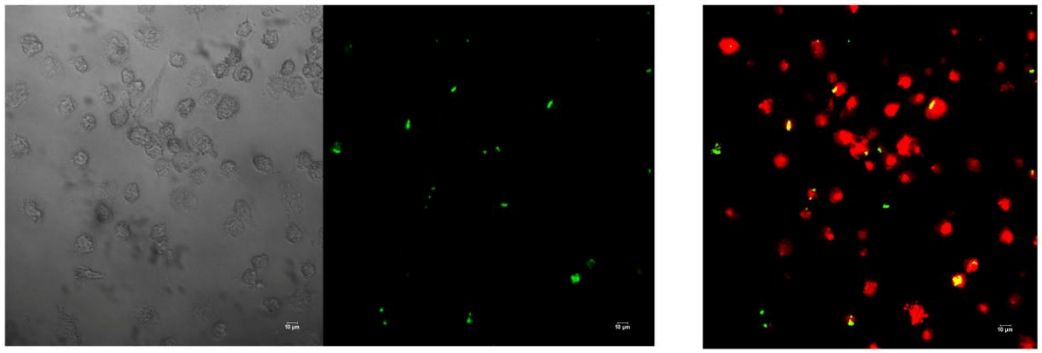

Control plasmid-transfected macrophage+H37Ra

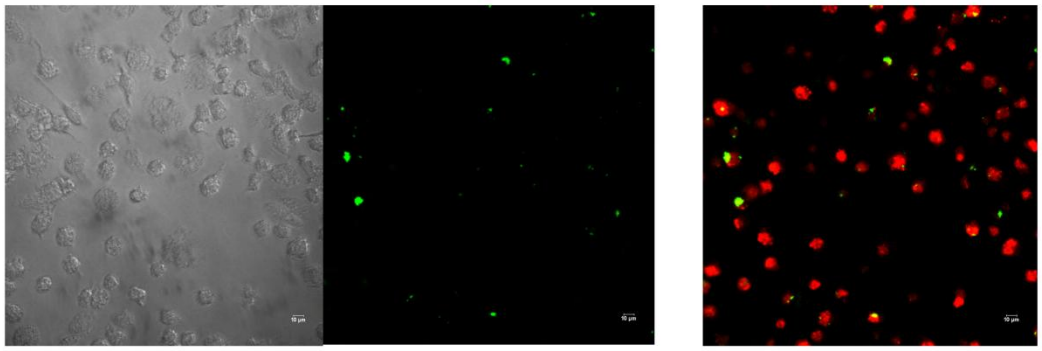

ESAT-6-transfected macrophage+H37Ra

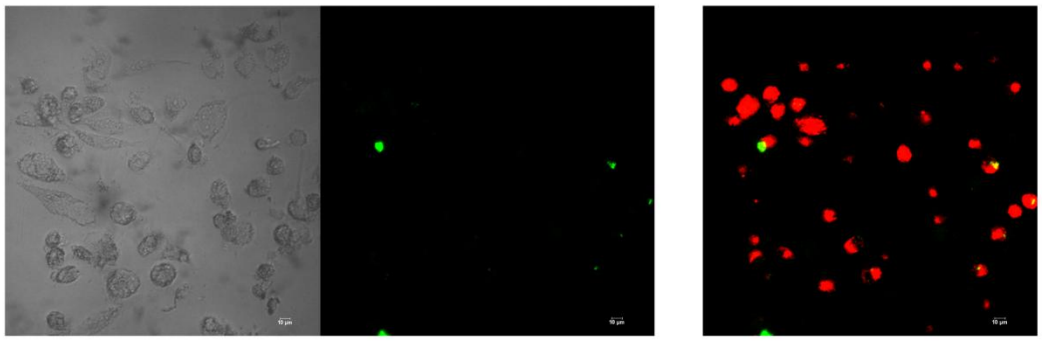

ESAT-6 M93A mutant-transfected macrophage+H37Ra

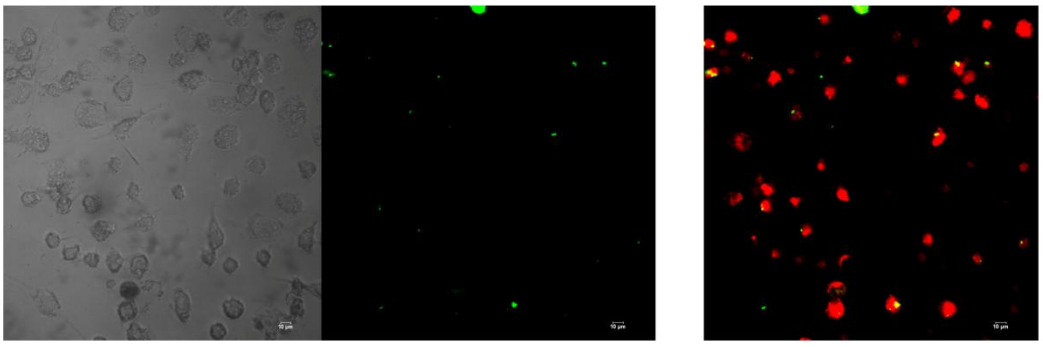

ESAT-6 M93C mutant-transfected macrophage+H37Ra

Fig. 16